Heliyon 10 (2024) e27199

Contents lists available at ScienceDirect

Heliyon

journal homepage: www.cell.com/heliyon

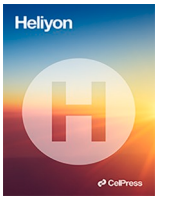

Research article

A novel mutation in *GTPBP3* causes combined oxidative phosphorylation deficiency 23 by affecting pre-mRNA splicing

Yanjun Wang [a,1], Juan He [a,1], Fangling Dong [a], Weihua Shou [b], Xingxing Feng [c], Ya Yang [a], Cuifen Li [a], Jingjing Wang [a], Bin Li [a,**], Shufang Xiao [a,*]

[a] *Pediatric Intensive Care Unit, Kunming Children's Hospital, Children's Hospital Affiliated to Kunming Medical University, Kunming, China*
[b] *Kunming Key Laboratory of Children Infection and Immunity, Yunnan Key Laboratory of Children's Major Disease Research, Yunnan Medical Center for Pediatric Diseases, Yunnan Institute of Pediatrics, Kunming Children's Hospital, Kunming, China*
[c] *Department of Clinical Laboratory, Kunming Children's Hospital, Children's Hospital Affiliated to Kunming Medical University, Kunming, China*

ARTICLE INFO

Keywords:
COXPD23
Novel *GTPBP3* mutation
Whole exome sequencing
Minigene
Mitochondrial diseases

ABSTRACT

Background: Combined Oxidative Phosphorylation Deficiency 23 (COXPD23) is a rare mitochondrial disease caused by mutations in the *GTPBP3* gene. The rare incidence of the disease and the high clinical heterogeneity pose challenges in making a precise diagnosis. Investigations into the rare COXPD23 patients are of pathophysiological and etiological value. In this study, we investigated the genotype-phenotype relationship in a COXPD23 patient from a Manchu family, with *GTPBP3* mutations.

Methods: Routine physical examinations, laboratory assays and imaging analyses were performed. The metabolic profiles of amino acids in blood, acylcarnitine in blood and organic acids in urine were used to determine the presence of inherited metabolic diseases. Genetic variations in the family were investigated using whole-exome sequencing and Sanger sequencing. Splicing disruption by a mutation was predicted and verified using a minigene assay.

Results: The patient presented with severe lactic acidosis, neurological symptoms, multiple symmetrical lesions in the brain and serious mitochondrial energy metabolism disturbances. The c.689A > C (p.Q230P) and c.809-1_809delinsA compound heterozygous mutations were detected in *GTPBP3*. The novel c.809-1_809delinsA mutation was located at the splicing site of exon 7 and intron 6 and multiple tools predicted that it would disrupt the normal splicing. The minigene assay proved that the novel mutation resulted in two aberrant transcripts that created premature termination codons.

Conclusions: The clinical manifestations, brain imaging change, mitochondrial metabolism disturbances and the detection and validation of the *GTPBP3* mutations expand the profile of COXPD23 and the pathogenic mutation spectrum. Our study improves the understanding of the pathophysiology and etiology of COXPD23.

* Corresponding author.
** Corresponding author.
E-mail addresses: kmlibin4761@sina.com (B. Li), xiaoshufang@etyy.cn (S. Xiao).
[1] These authors contributed equally to this study.

https://doi.org/10.1016/j.heliyon.2024.e27199
Received 1 February 2024; Accepted 26 February 2024
Available online 2 March 2024

1. Introduction

Abbreviations

COXPD23	Combined Oxidative Phosphorylation Deficiency 23
GTPBP3	GTP binding protein 3
HCM	hypertrophic cardiomyopathy
mt-tRNA	mitochondrial tRNA
MRI	brain magnetic resonance imaging
MS-MS	Tandem-mass-spectrometry
GC-MS	Gas chromatography-mass spectrometry
WES	Whole-exome sequencing
ACMG	American College of Medical Genetics and Genomics Standards
PTC	production of premature termination codon
CSF-TP	cerebrospinal fluid total protein
hs-cTnT	high-sensitivity cardiac troponin T
LDH	lactate dehydrogenase
CK	creatine kinase
AST	aspartic transaminase
ALT	alanine aminotransaminase
PT	prothrombin time
APTT	activated partial thromboplastin time
INR	international normalized ratio

Mitochondrial diseases, under the dual genetic control of nuclear and mitochondrial genomes, are a group of clinically heterogeneous, inherited metabolic disorders that are caused by the dysfunction of mitochondrial respiratory chain oxidative phosphorylation (OXPHOS) [1,2]. They represent by far the largest class of inborn defects of metabolism and are classified in accordance with the different pathogenic genes. The diseases mainly affect the brain, heart, liver and skeletal muscle, due to their high energy consumption. The high clinical heterogeneity of the diseases mainly manifests as a broad spectrum of pathophysiologic phenotypes, different disease progression, onset ages, clinical outcomes and corresponding severity [3]. The prevalence of mitochondrial diseases is estimated to be approximately 5/100000 to 15/100000 in children [1,4].

Combined Oxidative Phosphorylation Deficiency (COXPD) is a mitochondrial disease that is a severe autosomal recessive disorder. Online Mendelian Inheritance in Man (OMIM) has classified COXPD into 51 types (COXPD1-51). Of these, COXPD23 (MIM: 616198) is defined as being caused by mutations in the *GTPBP3* gene, (GTP binding protein 3, MIM: 608536), but its prevalence is not clear as only 19 COXPD23 patients have been reported, worldwide. The symptoms of these patients often emerged in early childhood and featured the onset of hypertrophic cardiomyopathy (HCM) and a series of neurological symptoms, such as hypotonia, developmental delay and intellectual disability [5,6]. Laboratory testing identified mitochondrial function defects such as lactic acidosis, impaired activity of respiratory chain complexes I and IV and defective translation of mitochondrial proteins [6]. Imaging examinations of the brain found abnormal lesions in the basal ganglia, thalamus and brain stem [6]. The severity of the disease varied significantly, from mortality in early infancy to teenage survival [7].

The human *GTPBP3* gene is a nuclear gene that maps to chromosome 19p13.11 and is composed of nine exons and eight introns (Fig. 1A) [8]. The GTPBP3 protein is composed of 492 amino acids and is found in the mitochondria. It functions as a mitochondrial GTP-binding protein and a mitochondrial (mt-) tRNA-modifying enzyme [8]. The protein is highly conserved and consists of a N-terminal domain, a GTPase domain (G domain) and a helical domain [9]. The GTPBP3 protein defect associated with COXPD23 inhibits taurine modification of mt-tRNA and causes mitochondrial translation damage [5].

Currently, 19 COXPD23 patients of multiple ethnicities have been reported. All are homozygous or compound heterozygous for 23 different variants in *GTPBP3* (Fig. 1B). Seven Chinese patients have been reported, with variable symptoms [7,8,10–12]. The rareness and high clinical heterogeneity pose challenges in the clinical diagnosis of the disease because there is no specific symptom, physical sign or single, reliable biomarker. Here, we described a patient from a Manchu ethnic minority family hospitalized in Kunming Children's Hospital. We analyzed the patient's clinical characteristics, routine laboratory test data, metabolic profiles and imaging examinations. We also investigated the potential genetic mutations that could induce the gene function defects. Investigations into the rare but precious cases of COXPD23 are anticipated to provide valuable information to guide clinical prognosis and genetic counseling in the future.

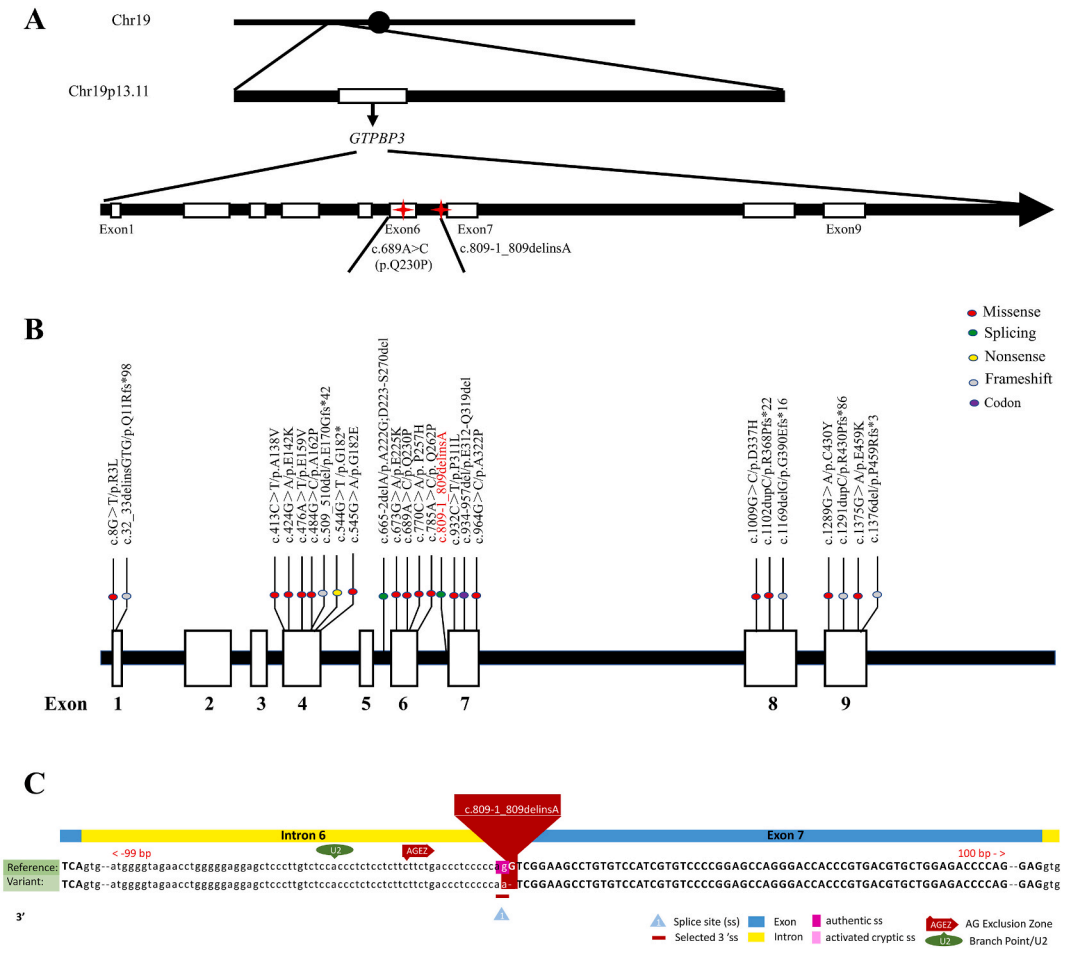

Fig. 1. **(A)** Structural diagram of *GTPBP3*. The *GTPBP3* gene is located on chromosome 19p13.11 and has nine exons and eight introns. **(B)** Distribution of *GTPBP3* mutations associated with COXPD23. The red arrow represents the novel mutation. **(C)** Schematic representation of the novel mutation position and base changes. The mutation involves a dinucleotide substitution at the boundary of intron 6 and exon 7, with the potential to affect splicing.

2. Materials and methods

2.1. Patient

The patient was a 5-month-old boy from a Chinese Manchu ethnic minority family, who visited Kunming Children's Hospital due to sudden convulsions. This study was approved by the Ethics Committee of Kunming Children's Hospital, Kunming, China (No.2023-05-003-01). Prior to sampling, we obtained informed consent from the parents of the patient. After admission, the patient underwent detailed clinical assessments and laboratory examinations. Peripheral blood samples were collected from the patient and his parents for hematological, serum biochemistry examination. Amino acid and carnitine detection were performed by Tandem-mass-spectrometry (MS-MS). A sequencing library was also prepared from the samples. Imaging examinations included color doppler ultrasonography of the liver, gallbladder, pancreas, spleen and kidney, cardiac ultrasonography and brain magnetic resonance imaging (MRI). The urine sample was analyzed for organic acids by Gas chromatography-mass spectrometry (GC-MS) and the peak identification was executed utilizing the Inborn Errors of Metabolism screening system (SHIMADZU, Kyoto, Japan).

2.2. Whole-exome sequencing (WES) and Sanger sequencing validation

We collected EDTA anti-coagulated venous blood from the patient and his parents. The genomic DNA was extracted using the QIAamp DNA Blood Mini Kit (Qiagen, Shanghai, China), following the manufacturer's protocol, and a genomic library was constructed using the Illumina standard protocol. The DNA was quantified with a Nanodrop 2000 (Thermal Fisher Scientific, DE). A minimum of 3 μg of DNA was used for the indexed Illumina libraries, in accordance with the manufacturer's protocol (MyGenostics, Inc., Beijing, China). The whole-exome target regions were captured by the GenCap kit (MyGenostics, Beijing, China) and the enriched library was

sequenced on a DNBSEQ-T7 sequencer (MGI, Shenzhen, China), for paired-end reads of 150 bp. The MGI sequencing adapters and low-quality reads (<80 bp) were filtered by cutadapt (http://cutadapt.readthedocs.io/). After quality control, the clean reads were mapped to the UCSC hg19 human reference genome using BWA [13] (http://bio-bwa.sourceforge.net/). The single nucleotide polymorphism (SNP) and insertion/deletion (InDel) variants were detected by GATK (https://software.broadinstitute.org/gatk/) HaplotypeCaller and then filtered for qualified variants using GATK VariantFiltration.

All candidate mutations were confirmed by Sanger sequencing. The target gene was sequenced on an ABI PRISM 3730 genetic analyzer (Applied Biosystems; Thermo Fisher Scientific). Sites of variation were identified through a comparison of DNA sequences with the corresponding GenBank (www.ncbi.nlm.nih.gov) reference sequences.

2.3. Prediction of the splicing effect of the mutation

The pathogenicity of each mutation was evaluated in strict accordance with the American College of Medical Genetics and Genomics (ACMG) Standards and Guidelines [14].

We used RDDC^{SC}(https://rddc.tsinghua-gd.org/search-middle?to=SplitToolModel), Varseak (https://varseak.bio/index.php) and SpliceAI (https://spliceailookup.broadinstitute.org/) for splice prediction.

2.4. Minigene splicing assay

2.4.1. Recombinant vector construction

Two commercial vectors, pcMINI and pcMINI-N (Bioeagle Biotech), were used to create recombinant minigene constructs with two experimental designs (Figs. 5A and 6A). In one design, the target fragment of wild type containing partial intron 6 (151 bp) -exon 7 (166bp) -partial intron 7 (732 bp) was amplified by nested PCR. In the other design, the target fragment of wild type containing exon 6 (144 bp) -intron 6 (167 bp) -exon 7 (166 bp) -partial intron 7 (678 bp) was amplified. We introduced the mutation that corresponds to c.809-1_809delinsA by site-directed mutagenesis. The wild type and mutant minigenes in the two designs were cloned into the pcMINI and pcMINI-N plasmids at the *Kpn*I and *Xho*I restriction sites, to generate four minigene constructs. All mutant constructs were

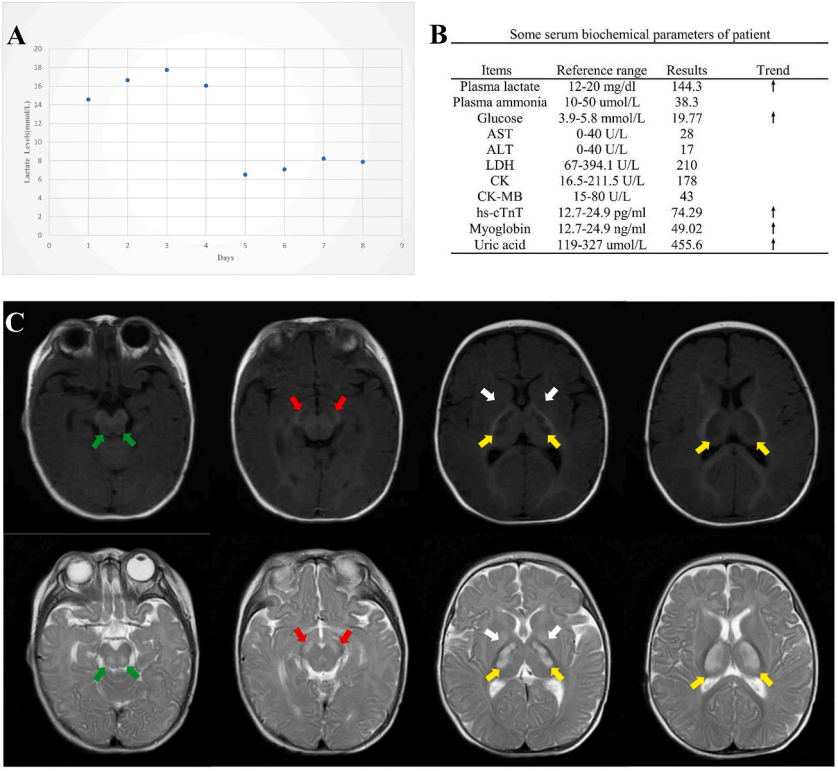

Fig. 2. The results of the clinical examinations. (**A**) Laboratory parameters of the patient. (**B**) Daily plasma lactate levels for the patient, from admission. CSF-TP, cerebrospinal fluid total protein; hs-cTnT, high-sensitivity cardiac troponin T; LDH, lactate dehydrogenase; CK, creatine kinase; AST, aspartic transaminase; ALT, alanine aminotransaminase; PT, prothrombin time; APTT, activated partial thromboplastin time; INR, international normalized ratio. (**C**) MRI images taken during hospitalization. The MRI demonstrated diffuse and symmetrical abnormal signals in bilateral cerebral foot (red arrowheads), posterior portion of the brain stem (green arrowheads), basal ganglia (white arrowheads) and thalamus (yellow arrowheads).

confirmed by sequencing. All the primers used in the nested PCR and mutagenesis are listed in Table S1.

2.4.2. Cell transfection

The recombinant vectors were transiently transfected into HeLa and 293T cell lines using Lipofectamine® 2000 (Thermo Fisher Scientific, Waltham, MA, CA).The transfected cells were cultured in DMEM medium for 48 h.

2.4.3. Minigene transcription analysis

The HeLa and 293T cells were harvested 48 h after transfection. Total RNA was extracted from cell samples using Trizol reagent (TaKaRa, DaLian, China), in accordance with the manufacturer's instructions. Reverse transcription was performed using the Hifair™ 1st Strand cDNA Synthesis SuperMix for qPCR (gDNA digester plus) kit (YEASEN, Shanghai, China). The PCR amplification was performed using the pcMINI-F/pcMINI-R and pcMINI-N-F/pcMINI-N-R flanking primers for the minigene. The PCR products were detected by agarose gel electrophoresis and each band on the gel was retrieved separately for Sanger sequencing, which was performed using an ABI 3130 DNA Analyzer (Applied Biosystems, Foster City, CA, USA). The Nonsense-mediated mRNA decay (NMD) pathway prediction tool (https://nmdpredictions.shinyapps.io/shiny/) was used to predict whether the abnormal transcripts would produce the corresponding truncated proteins.

A Urine organic acid profiles

Items	Reference range (umol/L)	Results	Trends
Lactic acid -2	0-4.7	1103.2	↑
Glycollic acid-2	0-2.2	17.5	↑
Oxalic acid-2	0	31.58	↑
2-hydroxybutyrate-2	0	193.48	↑
Glyoxylic acid-OX-2	0-6.1	20.18	↑
3-hydracrylicacid-2	0-1.1	43.17	↑
Pyruvic acid-OX-2	0-24.1	1023.12	↑
Valproic acid-1	0	4.97	↑
3-hydroxybutyrate-2	0-3.7	2222.45	↑
3-hydroxyisobutyrate-2	0-9	119.08	↑
2-hydroxyisovalerale-2	0	50.05	↑
3-hydroxyisovalerale-2	0-2.3	11.79	↑
2-keto-isovaleric acid-OX-2	0-0.1	19.19	↑
Hydroxy propionate-2	0-2.9	37.04	↑
3-hydroxyvaleric acid-2	0	10.02	↑
Acetoacetic acid-OX-2	0	13.39	↑
2-keto-3-methylpentanoic acid-OX-2	0	19.36	↑
Glyceric acid-3	0-0.8	17.54	↑
Phosphoric acid -3	0-43	218.31	↑
2-keto-Isocaproic acid-OX-2	0	36.13	↑
Acetylglycine-1	0-0.1	15.64	↑
Glyceric acid-3	0-1.6	5.94	↑
Fumaric acid-2	0-7.3	46.8	↑
Butyrylglycine-2	0-0.7	0.85	↑
Malic acid-3	0-0.7	7.13	↑
Adipic acid-2	0.5-5	14.91	↑
5-oxyproline-2	0-7.6	27.24	↑
7-hydroxyl-caprylic acid-2	0	0.76	↑
3-hydroxyglutaric acid-3	0	10.95	↑
2-hydroxyadipic acid-3	0-2	22.58	↑
Vanillic acid-2	0	16.43	↑
3-hydroxyoctanoic acid-3	0-4.8	10.78	↑
4-hydroxyphenyllactic acid-2	0-7	348.66	↑
4-hydroxyphenylpyruvic acid-OX-2	0-0.9	19.78	↑
Subyl glycine-2	0	0.98	↑
Palmitic acid-1	0-13.8	196.88	↑
3-hydroxycapric acid-3	0-4.4	16.36	↑
Uric acid-4	0-7.2	35.53	↑

C Blood amino acid and acylcarnitine profiles

Items	Reference range(umol/L)	Result	Trend
Alanine	60-300	412.186	↑
Arginine	1.5-25	1.094	↓
C4-OH carnitine	0.02-0.35	0.369	↑
C12-OH carnitine	0-0.1	0.51	↑

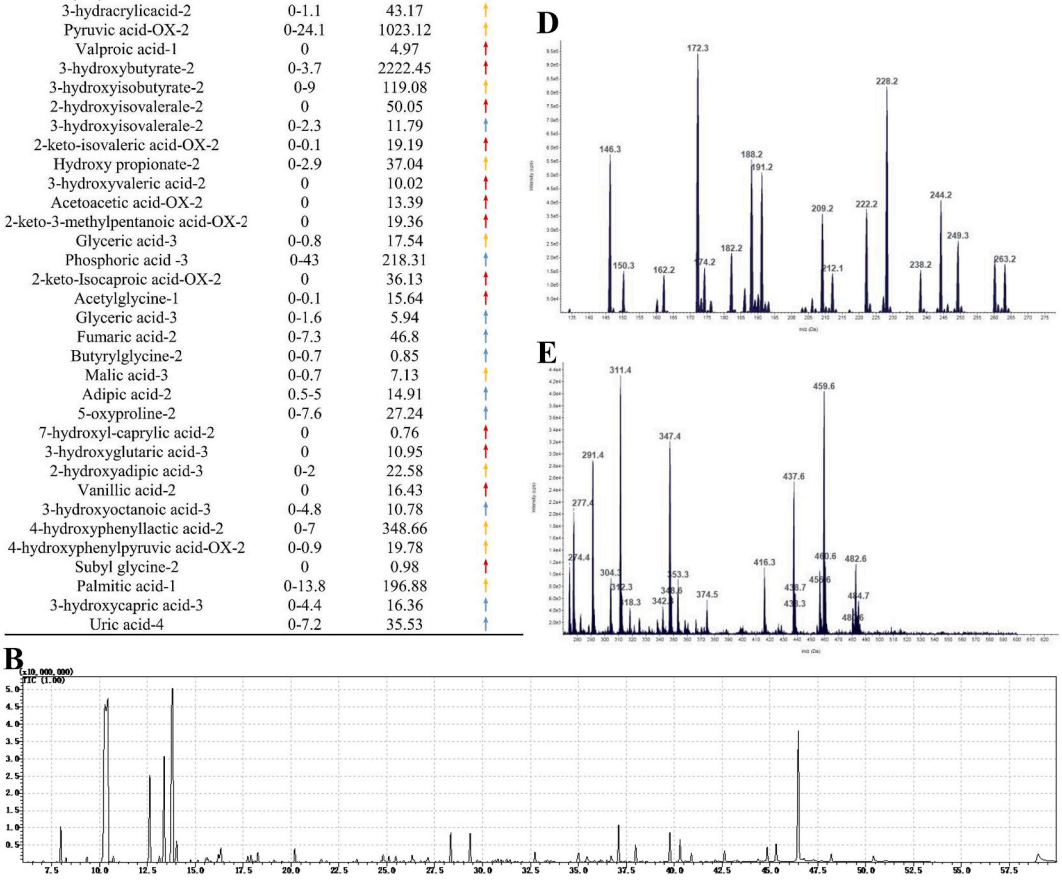

Fig. 3. Urine Organic Acid analysis and blood amino acid/carnitine screening.(**A**) Urine organic acid test results. (**B**) GC-MS profile of urine organic acid. (**C**) Blood amino acid test results. (**D**) Amino acid scan map. (**E**) Carnitine scan map. The fonts in red, orange and blue demonstrate an increase of more than a hundred times, ten times, and two times, respectively.

3. Results

3.1. Clinical and laboratory findings

The patient was a 5-month-old boy. He was the first child of the family and the pregnancy went to full-term. He was vaginally delivered, with a birth weight of 2900 g, and no asphyxia occurred at birth. The parents denied consanguineous marriage and a family history of similar disease. The mother's account indicated that the infant exhibited no discernible growth or developmental abnormalities and maintained a good state of health after birth. At five months of age, the patient suddenly developed convulsions and was admitted to Kunming Children's Hospital, China. The patient was suffering from hypotonia, respiratory failure and shock.

Arterial blood gas analysis showed an extreme lactate rise (Fig. 2A) and severe metabolic acidosis (pH 7.061, BE -26.5 mmol/L). The plasma lactate in the peripheral blood was consistently elevated (Fig. 2B). The routine laboratory tests (Fig. 2B) showed that high-sensitivity cardiac troponin T (hs-cTnT), glucose and uric acid were markedly elevated. The plasma ammonia, lactate dehydrogenase (LDH), creatine kinase (CK), creatine kinase isoenzyme-MB (CK-MB), aminotransferases and myoglobin were all within normal limits. Cerebrospinal fluid glucose was increased (6.08 mmol/L, normal range 2.8–4.5 mmol/L). An electroencephalogram (EEG) showed increased delta activity in the background. An electrocardiogram showed no obvious abnormality. Cardiac ultrasonography displayed tricuspid regurgitation. The brain MRI showed diffuse and symmetrical abnormal signals in the bilateral cerebral foot, posterior portion of the brain stem, basal ganglia and thalamus, showing T1W1 low/slightly low signal, T2W1 high signal, and T2 flair equal/

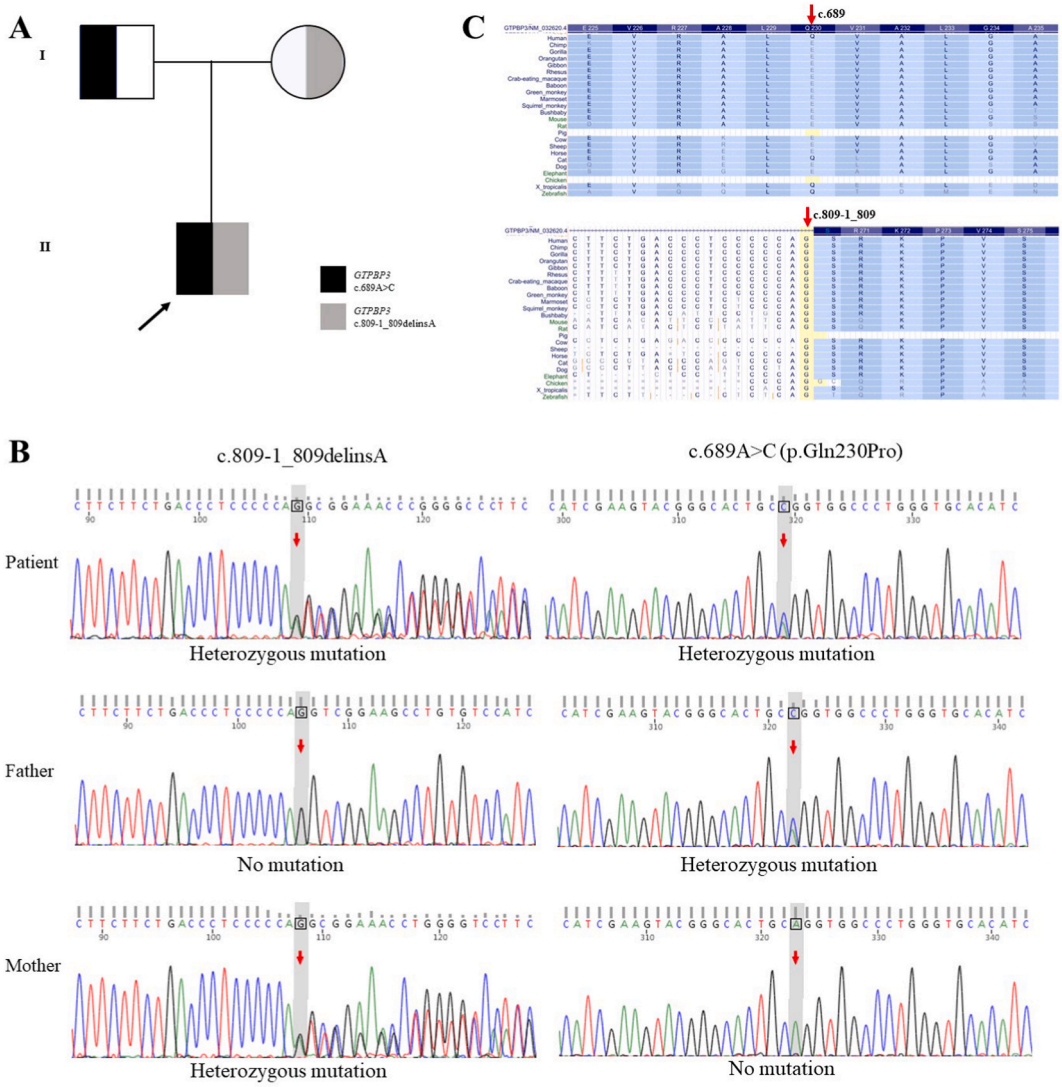

Fig. 4. The c.689A > C (p.Q230P) and c.809-1_809delinsA compound heterozygous mutations were detected in *GTPBP3*. **(A)** The pedigree for family. **(B)** Whole-exome sequencing and Sanger sequencing results for the patient and his parents for the two mutations. **(C)** Multispecies conservation analysis of the two variants.

slightly low signal (Fig. 2C). The results of the GC-MS showed an extremely increased level of urine lactate, in addition to varying degree of elevation of other organic acids (Fig. 3). The MS-MS metabolic analysis of a dried blood spot showed a mild increase in the level of alanine, C4–OH carnitine and C12–OH carnitine, in addition to a decreased level of arginine. Both the results of the GC-MS and the MS-MS analyses revealed profound mitochondrial energy metabolism disturbances in the patient.

We combined the clinical features of the patient and the above laboratory and imaging results to speculate that the boy was suffering from metabolic encephalopathy. However, the patient had no specific symptoms or physical signs, and there was no convincing genetic evidence in his family. This made making a rapid diagnosis challenging. The WES genetic analysis was further refined.

3.2. Detection and validation of mutations

A trio-WES analysis was performed on the patient and his parents to detect the potential genetic causes of the disease. The sequencing results revealed that the patient carried two heterozygous mutations, non-synonymous c.689A > C (p.Q230P) and c.809-1_809delinsA, in the *GTPBP3* gene. The c.689A > C missense mutation in exon 6 results in a change in amino acid 230, from glutamine to proline, with a rare minor allele frequency of 0.00004 in Asians, as reported in gnomAD. No record of the c.809-1_809delinsA mutation was found in the latest human gene mutation databases and we were unable to acquire information about its pathogenicity. In accordance with the ACMG guidelines, this mutation was preliminarily judged to be a likely pathogenic variant. The genotyping results for the parents revealed that the patient was a compound heterozygous carrier for the two *GTPBP3* mutations (Fig. 4A and B) and the c.689A > C (p.Q230P) mutation was inherited from his father. The novel c.809-1_809delinsA mutation was transmitted from his mother. The analysis of conservation showed that the amino acid at site c.689 is highly species specific, with glutamine found in humans and glutamic acid in other primates. In contrast, the amino acids at c.809-1_809 were highly conserved across multiple species, from fish to mammals (Fig. 4C).

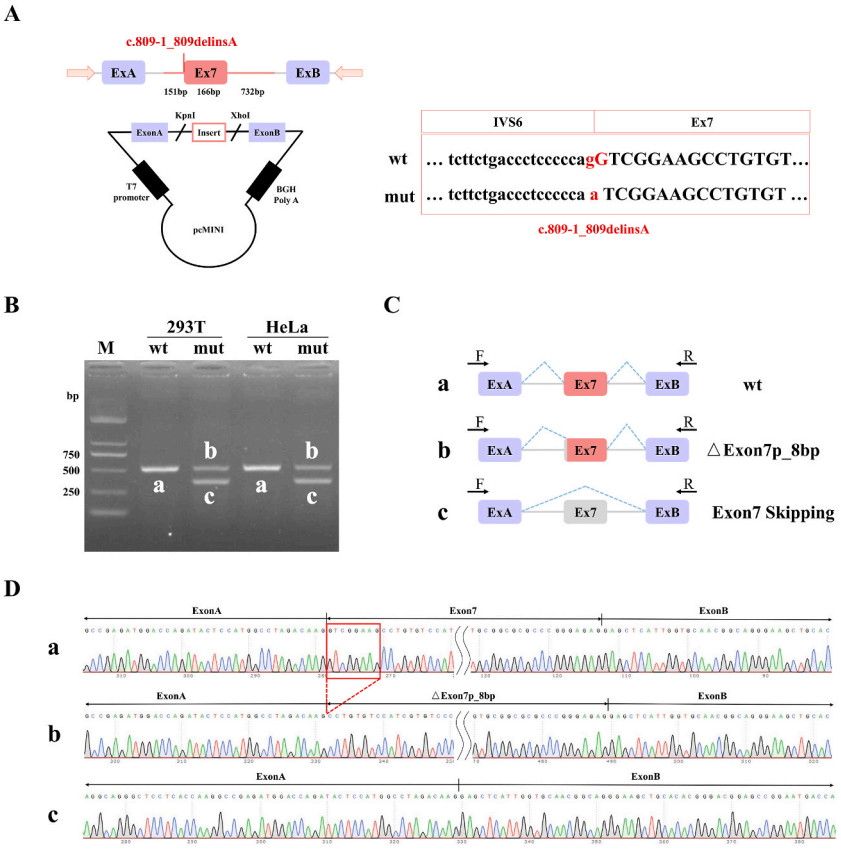

Fig. 5. Results of the pcMINI vector assay. **(A)** Diagram of the construction strategy for the minigene. **(B)** RT-PCR transcriptional analysis of agarose gel electrophoresis, in HeLa and 293T cells. M is the DNA marker. The wild type (wt) exhibited a single band, **a** (full); the mutant (mut) exhibited double bands, **b** (8-bp deletion) and **c** (exon 7 skipping). **(C)** Schematic diagram of minigene splicing. **(D)** The shear bands corresponding to the sequencing results.

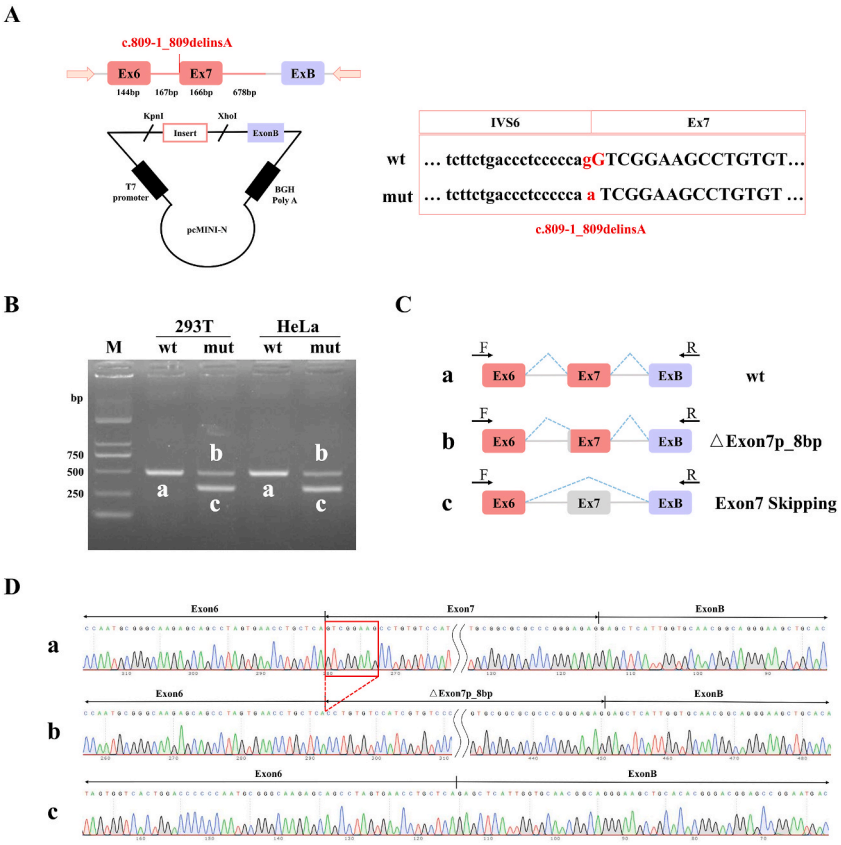

Fig. 6. Results of the pcMINI-N vector assay. **(A)** Diagram of the construction strategy for the minigene. **(B)** RT-PCR transcriptional analysis of agarose gel electrophoresis, in HeLa and 293T cells. M is the DNA marker. The wild type (wt) exhibited a single band, **a** (full); the mutant (mut) exhibited double bands, **b** (8-bp deletion) and **c** (exon 7 skipping). **(C)** Schematic diagram of minigene splicing. **(D)** The shear bands corresponding to the sequencing results.

3.3. Bioinformatics prediction for c.809-1_809delinsA in GTPBP3

Bioinformatics analyses were performed to predict the pathogenicity of the novel c.809-1_809delinsA mutation. This mutation involves a dinucleotide substitution at the boundary of intron 6 and exon 7, with the potential to affect splicing (Fig. 1C). The RDDC^{SC}, Varseak and SpliceAI programs consistently predicted a functional consequence of this mutation on the splicing of the *GTPBP3* transcripts. The RDDC^{SC} algorithm proposed that the mutation induces multiple splice patterns, such as a new acceptor, exon skipping or intron retention. These would allow for frameshifts and premature termination, and impair the function of the gene (Fig. S1). The Varseak and SpliceAI algorithms suggested that the original acceptor site may be destroyed by the mutation, threatening the normal splicing of the gene.

3.4. Verification of altered splicing by the minigene assay

We used the minigene constructs to investigate the effects of the mutation on splicing (Figs. 5A and 6A). The reverse transcription (RT)-PCR results (Figs. 5B and 6B) showed an identical transcription consequence due to the mutation in the two designs. In comparison to the wild type, the mutant construct consistently yielded two bands, which demonstrated that two different transcript isoforms were induced by altered splicing in the two cell lines. The transcripts generated by the wild type and mutant were confirmed by Sanger sequencing. The RT-PCR bands corresponded to three types of transcripts. The transcriptional product from the wild type came from normal splicing. The mutant type gave rise to two aberrant isoforms, one with a deletion of the first eight nucleotides of exon 7 and the other skipping the whole of exon 7 (Fig. 5C, D, 6C, 6D).

The minigene assays proved that the c.809-1_809delinsA mutation in *GTPBP3* can affect the normal splicing of mRNA. The results from pc-MINI and pc-MINI-N were consistent. The two abnormal transcripts can lead to a change in the protein. The nucleotide deletion to the left of exon 7 (c.809_816del) may cause the subsequent frameshift of a codon (p. Ser270Thrfs*14) and the production of a premature termination codon (PTC) during translation. This produces a truncated protein of 282 amino acids. The skipping of exon 7 (c.809_974del) can also completely change the subsequent reading frame of codon p. Arg271*, producing a PTC and a truncated protein of 270 amino acids. The abnormal pre-mRNAs, with PTCs, may be rapidly degraded by the NMD pathway, which plays a crucial

role in combating various diseases. We applied the NMD prediction tool to explore whether the abnormal transcripts would produce truncated proteins. We found that the p. Ser270Thrfs*14 and p. Arg271* variants did not produce truncated proteins but were predicted to be targeted for degradation by the NMD pathway.

4. Discussion

Combined Oxidative Phosphorylation Deficiency 23 is a rare mitochondrial disease caused by mutations in the *GTPBP3* nuclear gene. To date, seven studies, including our study, have described 20 cases of COXPD23 from 19 families. These families carry 25 variants in *GTPBP3* (Table S2). In 2014, Kopajtich et al. [6] first described 11 patients from Romania, Turkey, Arabia, India and Japan, with mutations in *GTPBP3*. They presented with lactic acidosis, HCM, neurological symptoms and combined respiratory chain complex deficiencies in skeletal muscle. The study also provided compelling evidence for the pathological role of mutant *GTPBP3* in mitochondrial disease. In 2019, Elmas et al. [15] reported a COXPD23 case from Turkey that was characterized by mental motor retardation, seizures, spasticity in lower extremities, severe learning disability and thrombocytopenia. Since 2021, five studies [7,8,10–12] have reported seven Chinese patients, from unrelated families, with COXPD23. Clinical manifestations included psychomotor developmental delay, seizures, hearing or vision impairment, hypotonia, dyspnea, lactic acidosis and HCM. In this report, we described one case with seizures, hypotonia, severe lactic acidosis, respiratory failure and shock.

Research has shown that the *GTPBP3* gene is associated with the modification of mt-tRNAs and aberrations in *GTPBP3* lead to mitochondrial dysfunction. For the tRNA maturation process to create cloverleaf structures that result in stable and properly functioning tRNAs, post-transcriptional modification is crucial [16]. The production of 5-taurinomethyluridine (τm^5U) is co-catalyzed by GTPBP3 and mitochondrial tRNA translation optimization 1 (MTO1) [9]. 5-taurinomethyluridine is located at the 34th wobble position of mt-tRNAs and is one type of mt-tRNA modification. Martinez-Zamora et al. [17] used a GTPBP3 stable-silencing model (shGTPBP3 cells) to investigate the phenotype caused by the GTPBP3 defect. The results showed that defective expression of *GTPBP3* triggers AMPK-mediated adaptive responses that may promote a shift from pyruvate to fatty acid oxidation, an uncoupling of glycolysis and oxidative phosphorylation. These metabolic alterations and the low ATP levels may negatively affect heart function. Chen et al. [18] used the gtpbp3 knockout zebrafish that was generated by the CRISPR/Cas9 system to demonstrate the aberrant mt-tRNA metabolism. The gtpbp3 knock-out zebrafish exhibited hypertrophy of cardiomyocytes and disarray of ventricles, which is consistent with the clinical phenotypes observed in patients with HCM, who carry *GTPBP3* mutations. Overall, *GTPBP3* has been identified as the causative factor underlying COXPD23.

All reported COXPD23 cases can be classified into mild or severe types, in accordance with the clinical phenotypes (Table S2). The mild type typically manifests in early childhood with mild encephalopathy, cardiomyopathy and hyperlactatemia. It exhibits a survival rate of up to 20 years of age. The 17 associated mutation sites in *GTPBP3* include c.8G > T, c.424G > A, c.476A > T, c.544G > T, c.545G > A, c.689A > C, c.770C > A, c.785A > C, c.932C > T, c.934-957del, c.964G > C, c.1102dupC, c.1169delG, c.1289G > A, c.1291dupC, c.1375G > A and c.1376del. The severe type typically manifests in infancy, presenting with acute metabolic decompensation and fatality due to heart failure and severe hyperlactatemia. The 11 associated mutation sites include c.32_33delinsGTG, c.413C > T, c.424G > A, c.484G > C, c.509_510del, c.665-2delA, c.673G > A, c.689A > C, c.809-1_809delinsA, c.964G > C and c.1009G > C. Four variants, c.424G > A, c.689A > C, c.785A > C and c.964G > C, were observed in both the mild and severe types. There were two homozygous (16.7%) individuals out of the 12 mild type patients and five homozygous (62.5%) individuals out of the eight severe type patients. This indicated that severe patients tend to carry homozygous mutations. In total, 25 mutations were found in *GTPBP3*. These included 16 missense mutations, five frameshift mutations, two splicing mutations, one codon change and one nonsense mutation. Six mutations were found in the homozygous form (c.770C > A, c.932C > T, c.32_33delinsGTG, c.424G > A, c.665-2delA and c.1009G > C), whilst the remainder were compound heterozygous mutations. Interestingly, all four patients with the c.785A > C variant were from unrelated Chinese families, which may indicate a different gene spectrum between different populations.

Although a growing number of studies have reported further COXPD23 cases with novel *GTPBP3* mutations, functional verification of the mutation sites has not been performed at the molecular level. In this study, we described a rare case of COXPD23 in a Chinese Manchu ethnic minority family. The patient developed the disease in infancy and died quickly. The results of tests on blood lactate levels, GC-MS analysis, MS-MS analysis and a brain MRI revealed that the patient had severe mitochondrial energy metabolism disturbances. We then performed WES and Sanger sequencing for further diagnosis. The c.689A > C (p.Q230P) and c.809-1_809delinsA compound heterozygous mutations were detected in *GTPBP3*. The c.689A > C mutation was first found in a Chinese patient with COXPD23 [7]. This missense mutation is in the critical domain of the GTPBP3 protein, the helical domain and the TrmE-type G domain [7]. In accordance with the ACMG guidelines, c.689A > C can be graded as 'likely pathogenic'. The c.809-1_809delinsA mutation is novel to our study. A minigene array was used to show that the mutation can affect the normal splicing of *GTPBP3* mRNA, leading to two transcripts. These include an 8-bp deletion (c.809_816del) on the left side of exon 7 and a skipping of exon 7, which results in a change in the subsequent read code box and the appearance of a PTC. Ultimately, the mutation may result in truncated proteins, which prevent the production of normal, functional proteins. However, in accordance with the NMD prediction, the two abnormal transcripts do not produce truncated proteins but are targeted for degradation by the NMD pathway. This indicates a complete loss of the GTPBP3 protein. Based on the above, the infant was diagnosed as having COXPD23 and the compound heterozygote c.689A > C and c.809-1_809delinsA mutations in the *GTPBP3* gene were thought to be the cause.

The disease exhibits significant interindividual variation in severity, ranging from early infancy fatality to survival into adulthood. This rare and clinically heterogeneous condition poses challenges for clinical diagnosis. If the patient shows early onset and the symptoms are cardiomyopathy, lactic acidosis and nervous system or multi-system symptoms, the disease is highly suspected and further screening using brain MRI analysis and testing for inherited metabolic diseases are recommended. Genetic testing is required

for a definitive diagnosis.

5. Conclusions

In conclusion, we reported a severe case of COXPD23 and identified a novel c.809-1_809delinsA mutation in the *GTPBP3* gene. The novel mutation affected the splicing of exon 7, leading to an 8-bp deletion on the left side of exon 7 and a skipping of exon 7, which resulted in the appearance of a truncated protein. The novel mutation expands the mutation spectrum of *GTPBP3* and improves our understanding of the molecular basis of COXPD23. Our study also improves the understanding of the pathophysiology and etiology of COXPD23.

Data availability statement

The data that support the findings of this study are available from the corresponding author upon reasonable request.

CRediT authorship contribution statement

Yanjun Wang: Conceptualization, Writing – original draft, Writing – review & editing. **Juan He:** Data curation, Investigation. **Fangling Dong:** Data curation. **Weihua Shou:** Formal analysis. **Xingxing Feng:** Methodology. **Ya Yang:** Methodology. **Cuifen Li:** Methodology. **Jingjing Wang:** Methodology. **Bin Li:** Supervision. **Shufang Xiao:** Validation.

Declaration of competing interest

The authors declare that they have no known competing financial interests or personal relationships that could have appeared to influence the work reported in this paper.

Acknowledgement

The work was supported by the National Natural Science Foundation of China (82160367), the Joint Special Fund for Basic Research from Yunnan Provincial Science and Technology Department and Kunming Medical University (202001AY070001-269), Yunnan Provincial Key specialty (Critical Care Medicine Department) construction project, the Sixth Cycle Key Discipline of Kunming (Critical Care Medicine Department) and Kunming high-level talents Training Special Project- Spring City famous doctor Special project. We also deeply appreciate the contribution of the patient and his parents to this work.

Appendix A. Supplementary data

Supplementary data to this article can be found online at https://doi.org/10.1016/j.heliyon.2024.e27199.

References

[1] L. Craven, C.L. Alston, R.W. Taylor, D.M. Turnbull, Recent Advances in mitochondrial disease, Annu Rev Genomics Hum Genet 18 (2017) 257–275.
[2] N. Yahata, Y. Matsumoto, M. Omi, N. Yamamoto, R. Hata, TALEN-mediated shift of mitochondrial DNA heteroplasmy in MELAS-iPSCs with m.13513G>A mutation, Sci. Rep. 7 (2017) 15557.
[3] F.G. Debray, M. Lambert, I. Chevalier, Y. Robitaille, J.C. Decarie, E.A. Shoubridge, B.H. Robinson, G.A. Mitchell, Long-term outcome and clinical spectrum of 73 pediatric patients with mitochondrial diseases, Pediatrics 119 (2007) 722–733.
[4] D. Skladal, J. Halliday, D.R. Thorburn, Minimum birth prevalence of mitochondrial respiratory chain disorders in children, Brain 126 (2003) 1905–1912.
[5] K. Murayama, M. Shimura, Z. Liu, Y. Okazaki, A. Ohtake, Recent topics: the diagnosis, molecular genesis, and treatment of mitochondrial diseases, J. Hum. Genet. 64 (2019) 113–125.
[6] R. Kopajtich, T.J. Nicholls, J. Rorbach, M.D. Metodiev, P. Freisinger, H. Mandel, A. Vanlander, D. Ghezzi, R. Carrozzo, R.W. Taylor, et al., Mutations in GTPBP3 cause a mitochondrial translation defect associated with hypertrophic cardiomyopathy, lactic acidosis, and encephalopathy, Am. J. Hum. Genet. 95 (2014) 708–720.
[7] Q. Zhang, Q. Ouyang, J. Xiang, H. Li, H. Lv, Y. An, Pathogenicity analysis of a novel variant in GTPBP3 causing mitochondrial disease and Systematic literature review, Genes 14 (2023).
[8] H.M. Yan, Z.M. Liu, B. Cao, V.W. Zhang, Y.D. He, Z.J. Jia, H. Xi, J. Liu, F. Fang, H. Wang, Novel mutations in the GTPBP3 gene for mitochondrial disease and characteristics of related phenotypic spectrum: the first three cases from China, Front. Genet. 12 (2021) 611226.
[9] G.X. Peng, Y. Zhang, Q.Q. Wang, Q.R. Li, H. Xu, E.D. Wang, X.L. Zhou, The human tRNA taurine modification enzyme GTPBP3 is an active GTPase linked to mitochondrial diseases, Nucleic Acids Res. 49 (2021) 2816–2834.
[10] F.Y. Yang Qian, Mitochondrial diseases associated with mutations in GTPBP3: a case report and literature review, Journal of Clinical Pediatric 39 (2021) 818–821.
[11] X.X. Zhao, X.Y. Wu, L.J. Xu, D. Wang, W. Jiang, L. Song, L. Kang, Mitochondrial cardiomyopathy caused by nuclear gene mutation: a case report and literature review, Molecular cardiology journal in China 21 (2021) 4387–4389.
[12] C. Wang, C. Yuan, Z. Ji, J. Yin, Z. Zhang, H. Zhang, B. Zheng, W. Zhou, S. Yang, Generation of patient-derived IPSC lines from a girl with Combined Oxidative Phosphorylation Deficiency 23 (COXPD23) caused by compound heterozygous GTPBP3 variants, Stem Cell Res. 61 (2022) 102775.
[13] H. Li, R. Durbin, Fast and accurate short read alignment with Burrows-Wheeler transform, Bioinformatics 25 (2009) 1754–1760.

[14] S. Richards, N. Aziz, S. Bale, D. Bick, S. Das, J. Gastier-Foster, W.W. Grody, M. Hegde, E. Lyon, E. Spector, et al., Standards and guidelines for the interpretation of sequence variants: a joint consensus recommendation of the American College of Medical genetics and genomics and the association for molecular Pathology, Genet. Med. 17 (2015) 405–424.
[15] M. Elmas, H. Yildiz, M. Erdogan, B. Gogus, K. Avci, M. Solak, Comparison of clinical parameters with whole exome sequencing analysis results of autosomal recessive patients; a center experience, Mol. Biol. Rep. 46 (2019) 287–299.
[16] L. Van Haute, S.F. Pearce, C.A. Powell, A.R. D'Souza, T.J. Nicholls, M. Minczuk, Mitochondrial transcript maturation and its disorders, J. Inherit. Metab. Dis. 38 (2015) 655–680.
[17] A. Martinez-Zamora, S. Meseguer, J.M. Esteve, M. Villarroya, C. Aguado, J.A. Enriquez, E. Knecht, M.E. Armengod, Defective expression of the mitochondrial-tRNA modifying enzyme GTPBP3 triggers AMPK-mediated adaptive responses involving complex I Assembly factors, uncoupling protein 2, and the mitochondrial pyruvate carrier, PLoS One 10 (2015) e0144273.
[18] D. Chen, Z. Zhang, C. Chen, S. Yao, Q. Yang, F. Li, X. He, C. Ai, M. Wang, M.X. Guan, Deletion of Gtpbp3 in zebrafish revealed the hypertrophic cardiomyopathy manifested by aberrant mitochondrial tRNA metabolism, Nucleic Acids Res. 47 (2019) 5341–5355.